THE JOURNAL OF BIOLOGICAL CHEMISTRY
Vol. 278, No. 23, Issue of June 6, pp. 21018–21023, 2003
Printed in U.S.A.

A Novel Lytic Peptide Composed of DL-Amino Acids Selectively Kills Cancer Cells in Culture and in Mice*

Received for publication, November 3, 2002, and in revised form, March 18, 2003
Published, JBC Papers in Press, March 19, 2003, DOI 10.1074/jbc.M211204200

Niv Papo‡, Michal Shahar‡, Lea Eisenbach§, and Yechiel Shai‡¶

From the ‡Departments of Biological Chemistry and §Immunology, The Weizmann Institute of Science, Rehovot, 76100 Israel

The high toxicity of most chemotherapeutic drugs and their inactivation by multidrug resistance phenotypes motivated extensive search for drugs with new modes of action. We designed a short cationic diastereomeric peptide composed of D- and L-leucines, lysines, and arginines that has selective toxicity toward cancer cells and significantly inhibits lung metastasis formation in mice (86%) with no detectable side effects. Its ability to depolarize the transmembrane potential of cancer cells at the same rate (within minutes) and concentration (3 μM), at which it shows biological activity, suggests a killing mechanism that involves plasma membrane perturbation. Confocal microscopy experiments verified that the cells died as a result of acute injury, swelling, and bursting, suggesting necrosis. Biosensor binding experiments and attenuated total reflectance-Fourier transform infrared spectroscopy using model membranes have substantiated its high selectivity toward cancer cells. Although this is an initial study that looked at tumor formation rather than the ability of the peptides to reduce established tumors, the simple sequence of the peptide, its high solubility, substantial resistance to degradation, and inactivation by serum components might make it a good candidate for future anticancer treatment.

Current anticancer chemotherapies that are based on alkylating agents, antimetabolites, and natural products respond incompletely; this is probably related to the development of drug resistance. Most chemotherapeutic agents also affect normal cells and consequently cause severe side effects (1). Thus, there is an urgent need to develop new classes of anticancer drugs with new modes of action that selectively target the cancer cells. A promising group under investigation includes cationic antimicrobial peptides, which are known to play an important role in the innate immunity of a diverse range of organisms, including insects, amphibians, and mammals (2). Most of these peptides have an amphipathic structure, and they preferentially bind and insert into negatively charged cell membranes. Consequently, destabilization of the membrane disturbs the electrolyte balance and induces the intracellular contents to leak, leading to cell death. In contrast to normal eukaryotic cells, which generally have low membrane potentials and whose outer leaflet almost exclusively consists of zwitterionic phospholipids, the prokaryotic and cancer cell membranes maintain large transmembrane potentials and have a higher content of anionic phospholipids on their outer leaflet. Many antimicrobial peptides therefore preferentially disrupt prokaryotic and cancer cell membranes rather than eukaryotic membranes (3).

Several *in vitro* studies were conducted with native all L-amino acid antimicrobial peptides with defined α-helical or β-sheet secondary structures (3). However, the use of native antimicrobial peptides *in vivo* is mainly limited due to the loss of their function in serum, partially because of enzymatic degradation and binding to serum components. Limited *in vivo* studies showed that some native and synthetic cationic antimicrobial peptides exhibited specific anticancer activity due to their ability to target mitochondria and trigger apoptosis; however, this occurred only when they were conjugated to homing domains (4, 5). Moreover, these peptides did not have a broad spectrum of activity. An *in vivo*/*ex vivo* study described the anti-ovarian cancer activity of the intraperitoneally injected antimicrobial peptide magainin and its analogs (6). However, their toxicity against normal cells and stability in serum have not been reported.

Recently, we developed a new family of antibacterial peptides composed of both L- and D-amino acids (diastereomers) with promising properties that allow their *in vivo* use (7). These peptides were derived from potent non-cell-selective lytic peptides by replacing a few L-amino acids with their D-enantiomers. The resulting diastereomeric peptides lost their cytotoxic effect against normal mammalian cells but preserved both their antibacterial activity and the ability to increase the permeability of negatively charged phospholipid membranes (7).

Here we show that a 15-amino-acid diastereomer of a lytic peptide, composed of only leucines, lysines, and arginines, with one-third of its sequence consisting of D-amino acids, is highly toxic against cancer cells and inhibits lung metastasis formation in mice with no detectable side effects. A 12-amino-acid diastereomer, whose antimicrobial activity is similar to that of the 15-mer peptide, failed to show anticancer activity. The mode of action of the 15-mer peptide was investigated by means of fluorescence confocal microscopy, surface plasmon resonance using biosensor and model membranes, and fluorescence spectroscopy.

EXPERIMENTAL PROCEDURES

Materials—4-Methyl benzhydrylamine resin and butyloxycarbonyl amino acids were purchased from Calbiochem-Novabiochem. Benzotriazolyl-*N*-oxy-tris(dimethylamino) phosphonium-hexafluorophosphate, egg sphingomyelin (SM),[1] bovine brain phosphatidylserine (PS), and

* This work was supported in part by the Israel Cancer Research Fund (ICRF) and Israel Cancer Association. The costs of publication of this article were defrayed in part by the payment of page charges. This article must therefore be hereby marked "*advertisement*" in accordance with 18 U.S.C. Section 1734 solely to indicate this fact.

¶ The Harold S. and Harriet B. Brady Professorial Chair in Cancer Research. To whom correspondence should be addressed: Dept. of Biological Chemistry, The Weizmann Institute of Science, Rehovot, 76100 Israel. Tel.: 972-8-9342711; Fax: 972-8-9344112; E-mail: Yechiel.Shai@weizmann.ac.il.

[1] The abbreviations used are: SM, sphingomyelin; PS, phosphatidylserine; PE, phosphatidylethanolamine; PC, phosphatidylcholine; $DiOC_6(3)$, 3,3′-dihexyloxacarbocyanine iodide; XTT, 2,3-bis[2-methoxy-4-nitro-5-sulfophenyl]-2H-tetrazolium-5-carboxanilide; PBS, phosphate-buffered saline; ATR, attenuated total reflectance; FTIR, Fourier transform infrared spectroscopy.

TABLE I
Lethal concentrations (LC_{50}) of $l^{3,10,13}$ $k^{7,8}$ $K_4R_2L_9$, $l^{3,4,8,10}$ K_5L_7 and mitomycin C

Results are the mean of three independent experiments each performed in duplicates, with standard deviation not exceeding 20%. ND, not determined.

Peptide designation	LC_{50} in μM			
	NIH-3T3 mouse fibroblasts	B16 F10 mouse melanoma	D-122 lung carcinoma	Hemolysis at 50 μM peptide
$l^{3,10,13}k^{7,8}K_4R_2L_9$	40	2.5	4.5	0
$l^{3,4,8,10}K_5L_7$	>100	100	>50	0
Mitomycin C	3	3	ND	0

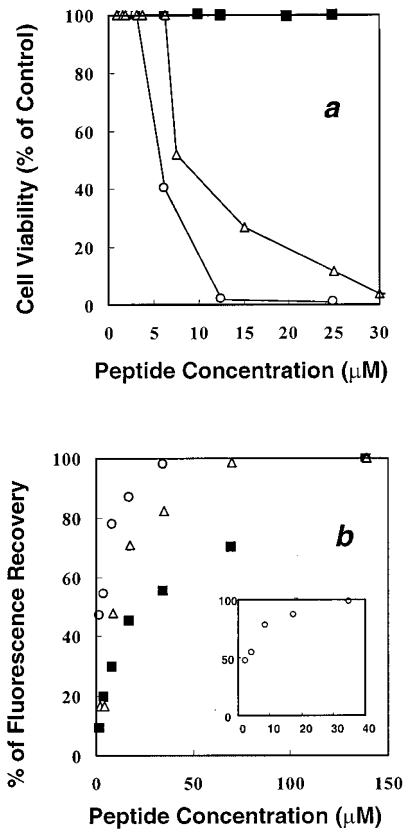

FIG. 1. **Activity against intact cells.** *a*, dose-dependent effect of $l^{3,10,13}k^{7,8}K_4R_2L_9$ in growth inhibition of the 3T3 (■), D122 (△), and B16 (○) cell lines. *b*, maximal dissipation of the diffusion potential in the 3T3 (■), D122 (△), and B16 (○) cell membrane, induced by $l^{3,10,13}k^{7,8}K_4R_2L_9$. For clarity, in the *inset*, we showed the change in the percentage of fluorescence recovery at low concentrations of diastereomer.

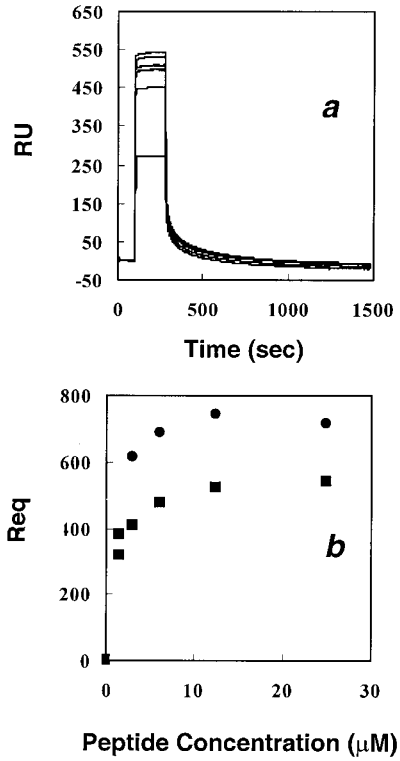

FIG. 2. **BIAcore binding studies.** *a*, sensograms of the binding between various concentrations of $l^{3,10,13}k^{7,8}K_4R_2L_9$ with the PC:SM:PE/cholesterol bilayers. *RU*, response unit. *b*, the relationship between the equilibrium binding response (*Req*) and the $l^{3,10,13}k^{7,8}K_4R_2L_9$ concentration in PC:SM:PE/cholesterol (■) or PC:SM:PE:PS/cholesterol (●) bilayers, using the BIAcore steady-state affinity model.

phosphatidylethanolamine (PE) (Type V, from *Escherichia coli*) were purchased from Sigma. Egg phosphatidylcholine (PC) was purchased from Lipid Products (South Nutfield, UK). Cholesterol (extra pure) was supplied by Merck. 3,3′-diethylthio-dicarbocyanine iodide and 3,3′-dihexyloxacarbocyanine iodide ($DiOC_6$(3)) were obtained from Molecular Probes (Eugene, OR). B16 F10 mouse melanoma, NIH-3T3 mouse fibroblasts, and the D122 Lewis lung carcinoma cell lines were purchased from the American Type Culture Collection (ATCC), Manassas, VA. Ten-to-twelve-week-old C57BL/6 male mice were provided by oLaC, Israel. All other reagents were of analytical grade.

Cell Cultures—B16 F10 cell lines were grown in RPMI 1640 medium supplemented with 10% fetal calf serum and antibiotics at 37 °C in a 5% CO_2 and 95% air humidified atmosphere. NIH-3T3 cell lines were grown in Dulbecco's modified Eagle's medium supplemented with 10% bovine calf serum and antibiotics as described above, and the D122 cell lines were also grown in Dulbecco's modified Eagle's medium supplemented with 10% fetal calf serum and antibiotics, as described above.

Peptide Synthesis and Purification—Peptides were synthesized by a solid phase method on a 4-methyl benzhydrylamine resin (8). The resin-bound peptide was cleaved by hydrogen fluoride and purified by reverse phase-high pressure liquid chromatography (RP-HPLC) as described elsewhere (7). The peptides were subjected to amino acid analysis and mass spectra to confirm their compositions.

Preparation of Small Unilamellar Vesicles—Small unilamellar vesicles were prepared by sonication of PC:SM:PE/cholesterol (4.5:4.5:1/1 w/w) or PC:SM:PE:PS/cholesterol (4.35:4.35:1:0.3/1 w/w) (3% PS) (7).

Cytotoxicity Assays (XTT Proliferation Assay)—Cells were seeded onto 96-well plates at a density of 1×10^4, 7×10^3, and 5×10^3 cells for 3T3, B16, and D122, respectively. Then the various concentrations of the peptide were added. The plate was then incubated for 24 h before adding to each well 50 μl of XTT reaction solution (sodium 3′-[1-(phenyl-aminocarbonyl)-3,4-tetrazolium]-bis(4-methoxy-6-nitro) benzene sulfonic acid hydrate and *N*-methyl dibenzopyrazine methyl sulfate, mixed in a proportion of 50:1). The optical density was read at 450 nm in an enzyme-linked immunosorbent assay plate reader after 2 h of incubation. Cell viability was determined relative to the control. All studies were done in triplicate.

Transmembrane Potential Depolarization Assay with the 3T3, B16, and D122 Cell Lines—3T3, B16, and D122 cells were incubated with 1 μM 3,3′-diethylthio-dicarbocyanine iodide, and the fluorescence intensity was recorded until a plateau was reached. The peptide, dissolved in PBS, was then added to 50 μl of the fluorescently labeled cells to reach a final volume of 100 μl (cells/well similar to the XTT assay). The resulting suspension was incubated with agitation for 60 min at 37 °C.

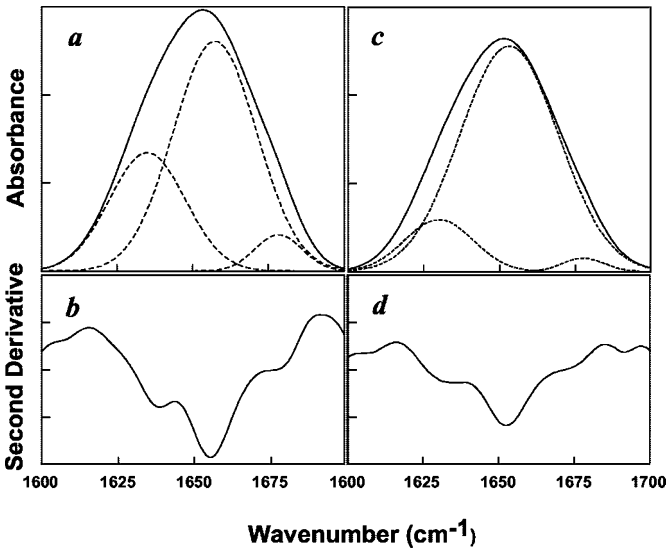

FIG. 3. **FTIR spectra deconvolution and second derivatives of the fully deuterated amide I band (1600–1700 cm^{-1}) of $l^{3,10,13}k^{7,8}K_4R_2L_9$ in the PC:PE/cholesterol (9:1/1 w/w) (*a* and *b*) and PC:PE:PS/cholesterol (4.85:4.85:0.3/1 w/w) (*c* and *d*) multibilayers.** The *broken lines* represent the fitted components. A 120:1 lipid/peptide molar ratio was used.

Membrane depolarization was monitored by observing the change in the intensity of fluorescence emission of the membrane potential-sensitive dye. The control for zero membrane depolarization (blank) consisted of fluorescently labeled cells suspended in PBS. 100% membrane depolarization was set as the difference in fluorescence intensity between 0 and 60 min after adding the dye to the cells.

Membrane Binding Analysis by Biosensor Based on Surface Plasmon Resonance—Biosensor experiments were carried out with a BIAcore X analytical system (Biacore, Uppsala, Sweden) using an L1 sensor chip, which forms a lipid bilayer. The L1 sensor chip is composed of long chain alkanethiol molecules that contain polar head groups, and when it is in contact with liposomes, a bilayer is formed (9). Peptide solutions (15 μl of PBS solution of 1 μM-100 μM peptide at a flow rate of 5 μl/min) were injected onto the lipid surface after PC:SM:PE/cholesterol (4.5:4.5:1/1 w/w) or PC:SM:PE:PS/cholesterol (4.35:4.35;1:0.3/1) lipids were applied to the chip surface (80 μl solution of 0.5 μM lipids at a flow rate of 2 μl/min).

Surface plasmon resonance detects changes in the reflective index of the surface layer of peptides and lipids in contact with the sensor chip. The curve of the resonance signal (response units), as a function of time, displays the progress of the interaction between the peptide and the lipid bilayer. Analysis of the peptide-lipid binding event was performed from a series of sensograms collected from seven different peptide concentrations in each case.

Secondary Structure Determination Using Attenuated Total Reflectance-Fourier Transform Infrared Spectroscopy (ATR-FTIR)—Spectra in lipids were obtained with a Bruker equinox 55 FTIR spectrometer equipped with a deuterated triglyceride sulfate detector and coupled with an ATR device, as described previously in detail (10). The results of four independent experiments were averaged.

Confocal Fluorescence Microscopy—Confocal images were obtained using an Olympus IX70 FV500 confocal laser scanning microscope. The $DiOC_6(3)$ and rhodamine system of filters were utilized. Unlabeled and $DiOC_6(3)$-labeled 3T3, B16, or D122 cells were placed on a coverslip, and a series of images was taken before and after the addition of unlabeled or rhodamine-labeled peptides, using oil immersion. The setting of the photomultipliers (gain and black level) was constant for the series of images. Care was taken so that any existing photobleaching did not compromise the interpretation, and laser irradiation and other means of illumination were prevented between images. The confocal images were obtained at a 12-bit resolution.

Lung Metastasis Model—Ten-to-twelve-week-old C57BL/6 male mice weighing 20–24 g were injected intravenously with 1×10^6 D122 lung carcinoma cells (11). After 24 h, the animals were randomly assigned into groups (n = 10 per group), and the vehicle (control) or the test compound was administrated. $l^{3,10,13}k^{7,8}K_4R_2L_9$ at 5 mg/kg or control (PBS, pH = 7.4) at 10 ml/kg was administered intravenously to the mice every day for 3 days in the first week and then once a week for the next 2 weeks for a total of five treatments in a period of 21 days. On day 28, the mice were sacrificed, and their lungs were removed and weighed to measure the extent of lung metastasis. The metastatic load was defined as the mean lung weight from mice injected with D122 cells minus the mean lung weight from five normal mice (178 ± 2 mg). The animal experimentation was reviewed and approved by the Institutional Animal Care and Use Committee.

RESULTS

Anticancer Activity in Cell Culture—We tested the potential of the 12-mer peptide $l^{3,4,8,10}K_5L_7$ (KLlLKLKlKlLK, small letters denote D-amino acids) and the 15-mer peptide $l^{3,10,13}k^{7,8}K_4R_2L_9$ (KLlRLLkkLlRLlLK) to inhibit the growth of the cancer and non-cancer cell lines. Both peptides would form an amphipathic helix in their all L-amino acid forms, as revealed by Schiffer and Edmundson wheel projection (12) (data not shown). Importantly, we found that the 15-mer $l^{3,10,13}k^{7,8}K_4R_2L_9$ had remarkable anticancer activity and selectivity toward cancer cells (~16-fold higher concentration for NIH-3T3 cells as compared with cancer cells) (Table I, Fig. 1*a*). In contrast, mytomycin C could not discriminate between the cancer and NIH-3T3 cells (Table I). The peptide was also not hemolytic toward human erythrocytes up to the maximum concentration tested (50 μM) (Table I). In contrast to the 15-mer, the 12-mer was not active against cancer cells despite the fact that its antimicrobial activity is high (data not shown). Additional mode of action studies were therefore conducted only with the active 15-mer.

Transmembrane Potential Depolarization Assay with the 3T3, B16, and D122 Cell Lines—To test whether the observed anticancer activity is related to cell membrane disruption, we performed transmembrane potential depolarizing experiments with the 3T3, B16, and D122 cells. Importantly, the data revealed a direct correlation between the LC_{50} (concentration of the peptide that lyses 50% of the cells) values for all cells (Table I) and the dose-dependent dissipation of their transmembrane potential (Fig. 1*b*), suggesting that one of the targets of the peptide is the cell membrane. As expected, the peptide could not dissipate the transmembrane potential of erythrocytes, in agreement with its non-hemolytic activity (data not shown). In addition, the peptide was also stable to enzymatic degradation by trypsin, proteinase-K, and elastase and was monomeric both in solution and when bound to cell membranes (data not shown).

Peptide Affinity to Lipid Bilayers Measured by Surface Plasmon Resonance—PC:SM:PE/cholesterol and PC:SM:PE:PS/cholesterol lipids, which mimic the membrane bilayers of non-tumorigenic and cancer cells, respectively, were absorbed onto the L1 chip. The peptide concentrations used in all assays were 3.125, 6.25, 12.5, 25, 50, and 100 μM. The response unit signal intensity increased as a function of the concentration of the peptide, indicating that the amount of peptide bound to the lipids is proportional to the increase in peptide concentration (Fig. 2*a*). Our system reached binding equilibrium while the samples were injected, and therefore, the affinity constant could be calculated from the relationship between the equilibrium binding response (Req) and the peptide concentration (C), using a steady-state affinity model (Fig. 2*b*). The affinity constants, defined as the ratio of the association (k_a) and dissociation (k_d) rate constants ($k_A = k_a/k_d$), were calculated and found to be 5.9×10^4 for the zwitterionic PC:SM:PE/cholesterol lipids and 6.2×10^5 for the anionic PC:SM:PE:PS/cholesterol lipids. These results clearly show a 10-fold higher affinity for the peptide toward anionic lipids than with the zwitterionic ones.

Secondary Structure of the Peptide in PC:PE/Cholesterol and PC:PE:PS/Cholesterol Phospholipid Membranes as Determined by FTIR Spectroscopy—ATR-FTIR was used to determine the

TABLE II

Assignment, wavenumbers (v), and relative areas of the component peaks determined from the deconvolution of the amide I bands of $l^{3,10,13}k^{7,8}K_4R_2L_9$ incorporated into multibilayers

A 120:1 lipid: peptide molar ratio was used. The results are the average of four independent experiments.

Structure assignment	PC:PE/Cholesterol		PC:PE:PS/Chol	
	v	Area	v	Area
	cm^{-1}	%	cm^{-1}	%
β-sheet	1630 ± 3	13 ± 2	1628 ± 2	17 ± 3
Distorted/3_{10}-helix	1656 ± 1	84 ± 3	1656 ± 1	83 ± 3
Turns/antiparallel β-Sheet	1677 ± 2	3 ± 1		

secondary structure of the 15-mer when bound to the PC:PE/cholesterol (9:1/1 w/w) or PC:PE:PS/cholesterol (4.85:4.85:0.3/1 w/w) multibilayers, which are phospholipid compositions typical of the outer leaflet of non-tumorigenic cells (13) or the outer leaflet of cancer cells (14), respectively. The lipid SM was not used because it has a strong signal in the amide I region, but the results in the functional assays were similar when using liposomes with or without SM. Our assignment of the different secondary structures was the same as that described previously (15–20). The data revealed that the peptide adopts predominantly distorted/dynamic helical structures in both types of lipids (Fig. 3 and Table II). Moreover, the phospholipid membrane was well ordered and was predominantly in a liquid-crystalline phase like biological cell membranes (data not shown) (21, 22).

Treating the lipid membrane with the 15-mer for a very short period (1 min) resulted in no change in the order of the alkyl chains of the lipid. However, after a longer incubation time (10 min), the order of the alkyl chains was changed significantly (data not shown).

The 15-mer Selectively Binds and Lyses Cancer Cells as Observed by Using Confocal Fluorescence Microscopy—The 15-mer was labeled with rhodamine at its N terminus without affecting its anticancer activity. When rhodamine-labeled 15-mer (2.5 μM) was added separately to 3T3 (Fig. 4*a*), B16 (Fig. 4*b*) cells, and D122 cells (figure not shown), we observed that the peptide was bound preferentially to the cancer cells. We further confirmed selective binding by placing together 3T3 cells that had been labeled with the green dye $DiOC_6(3)$ with unlabeled cancer cells. The addition of rhodamine-labeled 15-mer resulted in specific labeling (*red*) of only the cancer cells (Fig. 4*c*). We also found that the green dye $DiOC_6(3)$ does not interfere with the binding of rhodamine-labeled 15-mer (data not shown).

To test the lytic effect of the 15-mer, it was incubated with cancer cells at its LC_{50}, and images were taken. Fig. 5 shows such images for B16 cells after their treatment for 2, 6, and 10 min (Fig. 5, *a–c*, respectively). The data clearly show that the cells died as a result of acute injury, swelling, and bursting. Further experiments with rhodamine-labeled peptide revealed that it bound predominantly to the cell membrane (Fig. 5*d*) followed by complete removal of all the cytoplasmic content, leaving only the nucleus intact (Fig. 5*e*). Interestingly, the peptide could not penetrate into the nucleus.

The 15-mer Inhibits Metastasis Formation in Mice—Finally, we analyzed the *in vivo* anti-tumor activity of the 15-mer by assessing its ability to inhibit the formation of D122 lung tumors in C57BL/6 mice when injected intravenously. During the experiment, the mice were monitored continuously for clinical signs of toxicity. It was noted that the animals exhibited a reduction in spontaneous motor activity after the peptide was injected, but the symptoms disappeared within about 1–2 h. After the fourth injection of the peptide, 1 out of 10 mice died. Nevertheless, throughout the assay period, the animals that had been treated with the peptide were in good condition, did not express any signs of weakness, and maintained their body weight (data not shown). At the end of the experiment, we found that mice that had been injected with D122 lung carcinoma cells and treated with the 15-mer had markedly decreased lung weight (265 ± 33 mg) as compared with the control group injected with PBS (878 ± 69 mg) (Fig. 6, *a–d*). Moreover, the metastatic load was decreased by 86% in the group treated with the 15-mer as compared with the control group. The experiments were also performed with B16 melanoma cells (a group of five mice), and the results were similar to those obtained with D122 cells (data not shown).

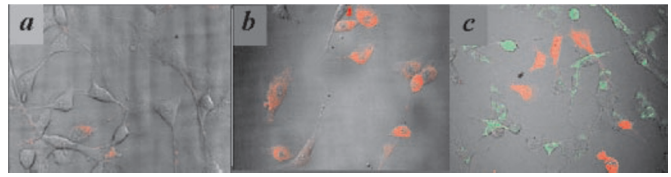

FIG. 4. **Confocal laser scanning microscopy images.** *a*, 3T3 cells treated with 2.5 μM rhodamine-labeled $l^{3,10,13}k^{7,8}K_4R_2L_9$. *b*, B16 melanoma cells treated with 2.5 μM rhodamine labeled $l^{3,10,13}k^{7,8}K_4R_2L_9$. *c*, images of 3T3 cells that were first labeled with the dye $DiOC_6(3)$ (*green*), and then mixed with unlabeled B16. Then, rhodamine-labeled peptide was added to the cell mixture.

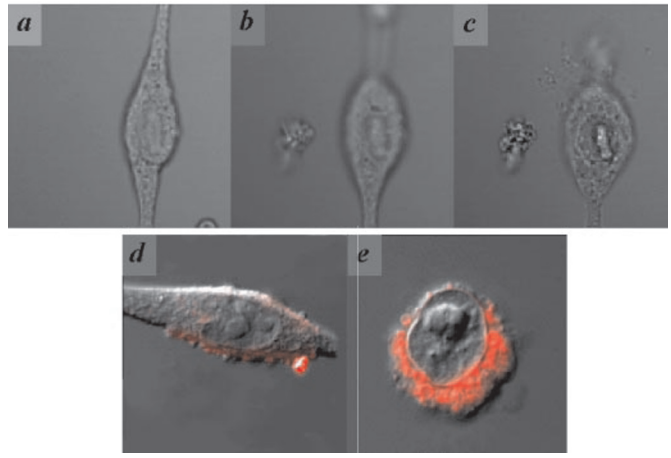

FIG. 5. **Confocal laser scanning microscopy images of B16 cells.** *a*, 2-min treatment with 2.5 μM of the 15-mer. *b*, 6-min treatment. *c*, 10-min treatment. *d* and *e*, B16 cells treated with 2.5 μM rhodamine-labeled peptide for 2 min (*d*) and for 15 min (*e*).

DISCUSSION

The most interesting finding is that the 15-mer is highly selectively toxic toward cancer cell lines (Table I, Fig. 1). Moreover, the 15-mer is highly active in inhibition of lung and B16 melanoma metastasis in mice (Fig. 6). In fact, it decreased the lung metastatic load in C57BL/6 mice by 86% without causing any noticeable weakness or loss of body weight in the animals at the end of the experiment. Although given intravenously, a histopathological evaluation revealed that the 15-mer (5 mg/

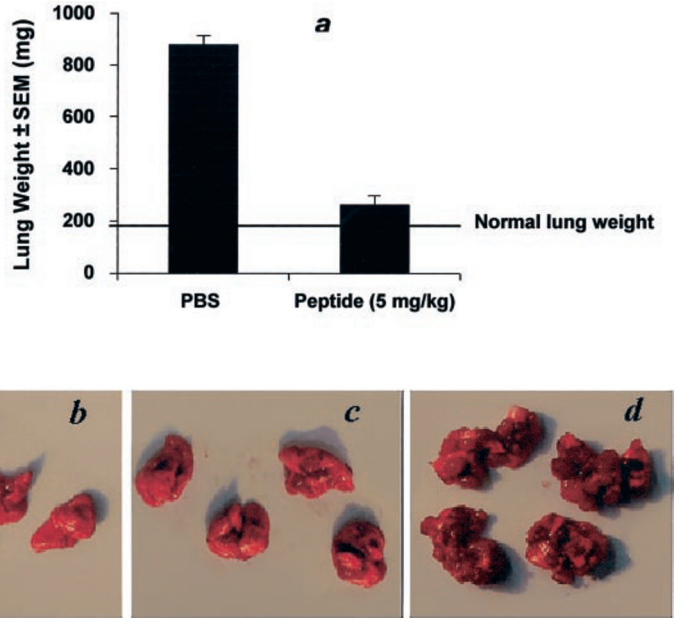

FIG. 6. **Reduction in lung metastatic load in C57BL/6 mice treated with $l^{3,10,13}k^{7,8}K_4R_2L_9$.** *a*, the lung weight of D122 lung tumor-bearing mice treated with $l^{3,10,13}k^{7,8}K_4R_2L_9$ or vehicle control. $p < 0.005$, Student's *t* test. The horizontal line indicates the average level of normal lung weight (178 mg). *b*, lungs of normal mice. *c* and *d*, lungs of mice injected with D122 lung tumor and treated with $l^{3,10,13}k^{7,8}K_4R_2L_9$ (*c*) or vehicle control (*d*).

kg) did not cause any damage to any of the organs of the mice (data not shown). Mitomycin, which served as a control, killed both cancer and the NIH-3T3 cells at a similar concentration.

The selective activity of the 15-mer toward cancer cells correlates with its 10-fold higher affinity toward anionic as compared with zwitterionic phospholipid membranes, as revealed by the biosensor studies. This suggests that the selective action of the 15-mer is a consequence of selective binding, mainly governed by electrostatic interactions. The high affinity of the peptide toward anionic phospholipids was reflected in its rapid and selective binding to cancer cells observed *in vitro* by using confocal microscopy (Fig. 4). Furthermore, a short time after binding, the cells died as a result of acute injury, swelling, and bursting, suggesting necrosis (Fig. 5). The finding that the 15-mer depolarized the cancer transmembrane potential of the cells at the same rate (within minutes) and concentration (3 μM) at which it showed biological activity suggests the existence of a killing mechanism that involves plasma membrane perturbation. Interestingly, the peptide was able to remove all the cytoplasmic parts of the cell but could not insert and destroy the nucleus, which remained apparently intact after the death of the cell (Fig. 5).

Structural studies using ATR-FTIR spectroscopy revealed that the 15-mer has an unordered structure in solution (data not shown). However, membrane binding forced the peptide to adopt a predominantly distorted/dynamic helical structure, which is sufficient to destabilize membranes (Table II, Fig. 3). More specifically, the ATR-FTIR studies showed that the peptide initially binds onto the surface and then is inserted into the membrane and destabilizes its packing. In other words, the initial interaction and selective recognition are electrostatically driven, but after binding, hydrophobic interactions play an important role, due to the partial amphipathic structure of the peptide.

Diastereomeric peptides have several advantages over the known all L- or all D-lytic peptides. First, they lack the diverse pathological and pharmacological effects induced by α-helical cytolytic peptides (23). Second, many amphipathic α-helical peptides bind to calmodulin and elicit several cell responses. Diastereomers with disrupted α-helical structure are not expected to bind to calmodulin. Third, they are amendable to controlled enzymatic degradation depending on the position of the D-amino acids. Fourth, the antigenicity of short fragments containing DL-amino acids is altered in comparison with their wholly L- or D-amino acid parent molecules (24), and fifth, anticancer activity is associated with total lysis of the cancer cells, as shown by confocal microscopy. Therefore, the cells should not easily develop resistance to drugs that trigger such a destructive mechanism.

Our study is preliminary, and there is a substantial need to expand it to a broader spectrum of cancer cells. Indeed, we looked at tumor formation rather than the ability of the peptides to reduce established tumors. Studies using an established xenograft model of human breast cancer cells are in progress. Nevertheless, the 15-mer, because of its unique mode of action, broad spectrum of anticancer activity, rapid and direct biological activity, and stability toward enzymatic degradation, is expected to complement existing therapeutic regimens without eliciting multidrug resistance mechanisms or enhancing genotoxic processes in normal tissues.

Acknowledgments—We thank E. Vadai for help in the *in vivo* experiments, V. Kiss for technical assistance in microscopy studies, Dr. A. Rabinkov for assistance in the Biacore studies, and S. G. Peisajovich for comments and critical reading of the manuscript.

REFERENCES

1. Smith, L. L., Brown, K., Carthew, P., Lim, C. K., Martin, E. A., Styles, J., and White, I. N. (2000) *Crit. Rev. Toxicol.* **30,** 571–594
2. Boman, H. G. (1995) *Annu. Rev. Immunol.* **13,** 61–92
3. Chan, S. C., Yau, W. L., Wang, W., Smith, D. K., Sheu, F. S., and Chen, H. M. (1998) *J. Pept. Sci.* **4,** 413–425
4. Chen, Y., Xu, X., Hong, S., Chen, J., Liu, N., Underhill, C. B., Creswell, K., and Zhang, L. (2001) *Cancer Res.* **61,** 2434–2438
5. Ellerby, H. M., Arap, W., Ellerby, L. M., Kain, R., Andrusiak, R., Rio, G. D., Krajewski, S., Lombardo, C. R., Rao, R., Ruoslahti, E., Bredesen, D. E., and Pasqualini, R. (1999) *Nat. Med.* **5,** 1032–1038
6. Baker, M. A., Maloy, W. L., Zasloff, M., and Jacob, L. S. (1993) *Cancer Res.* **53,** 3052–3057
7. Oren, Z., Hong, J., and Shai, Y. (1997) *J. Biol. Chem.* **272,** 14643–14649
8. Merrifield, R. B., Vizioli, L. D., and Boman, H. G. (1982) *Biochemistry* **21,** 5020–5031
9. Mozsolits, H., Wirth, H. J., Werkmeister, J., and Aguilar, M. I. (2001) *Biochim. Biophys. Acta* **1512,** 64–76
10. Oren, Z., and Shai, Y. (2000) *Biochemistry* **39,** 6103–6114
11. Porgador, A., Bannerji, R., Watanabe, Y., Feldman, M., Gilboa, E., and Eisenbach, L. (1993) *J. Immunol.* **150,** 1458–1470
12. Schiffer, M., and Edmundson, A. B. (1967) *Biophys. J.* **7,** 121–135
13. Verkleij, A. J., Zwaal, R. F., Roelofsen, B., Comfurius, P., Kastelijn, D., and Deenen, L. L. v. (1973) *Biochim Biophys Acta* **323,** 178–193
14. Zwaal, R. F., and Schroit, A. J. (1997) *Blood* **89,** 1121–1132
15. Jackson, M., and Mantsch, H. H. (1995) *Crit. Rev. Biochem. Mol. Biol.* **30,** 95–120
16. Tatulian, S. A., Biltonen, R. L., and Tamm, L. K. (1997) *J. Mol. Biol.* **268,** 809–815
17. Rothemund, S., Beyermann, M., Krause, E., Krause, G., Bienert, M., Hodges,

R. S., Sykes, B. D., and Sonnichsen, F. D. (1995) *Biochemistry* **34,** 12954–12962
18. Krause, E., Beyermann, M., Dathe, M., Rothemund, S., and Bienert, M. (1995) *Anal. Chem.* **67,** 252–258
19. Sharon, M., Oren, Z., Shai, Y., and Anglister, J. (1999) *Biochemistry* **38,** 15303–15316
20. Dwivedi, A. M., and Krimm, S. (1984) *Biopolymers* **23,** 923–943
21. Cameron, D. G., Casal, H. L., Gudgin, E. F., and Mantsch, H. H. (1980) *Biochim. Biophys. Acta* **596,** 463–467
22. Ishiguro, R., Kimura, N., and Takahashi, S. (1993) *Biochemistry* **32,** 9792–9797
23. Abu-Raya, S., Bloch-Shilderman, E., Shohami, E., Trembovler, V., Shai, Y., Weidenfeld, J., Yedgar, S., Gutman, Y., and Lazarovici, P. (1998) *J. Pharmacol. Exp. Ther.* **287,** 889–896
24. Benkirane, N., Friede, M., Guichard, G., Briand, J. P., Van, R. M., and Muller, S. (1993) *J. Biol. Chem.* **268,** 26279–26285